

Orbital structure of FeTiO₃ ilmenite investigated with polarization-dependent X-ray absorption spectroscopy and band structure calculations

S. W. Chen, M. J. Huang, P. A. Lin, H. T. Jeng, J. M. Lee et al.

Citation: *Appl. Phys. Lett.* **102**, 042107 (2013); doi: 10.1063/1.4789992

View online: <http://dx.doi.org/10.1063/1.4789992>

View Table of Contents: <http://apl.aip.org/resource/1/APPLAB/v102/i4>

Published by the [American Institute of Physics](#).

Additional information on *Appl. Phys. Lett.*

Journal Homepage: <http://apl.aip.org/>

Journal Information: http://apl.aip.org/about/about_the_journal

Top downloads: http://apl.aip.org/features/most_downloaded

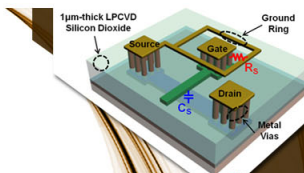
Information for Authors: <http://apl.aip.org/authors>

ADVERTISEMENT



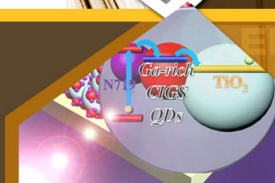
**EXPLORE WHAT'S
NEW IN APL**

SUBMIT YOUR PAPER NOW!



SURFACES AND INTERFACES

Focusing on physical, chemical, biological, structural, optical, magnetic and electrical properties of surfaces and interfaces, and more...



ENERGY CONVERSION AND STORAGE

Focusing on all aspects of static and dynamic energy conversion, energy storage, photovoltaics, solar fuels, batteries, capacitors, thermoelectrics, and more...

Orbital structure of FeTiO₃ ilmenite investigated with polarization-dependent X-ray absorption spectroscopy and band structure calculations

S. W. Chen,¹ M. J. Huang,¹ P. A. Lin,^{2,3} H. T. Jeng,^{2,3} J. M. Lee,¹ S. C. Haw,¹ S. A. Chen,¹ H. J. Lin,¹ K. T. Lu,¹ D. P. Chen,⁴ S. X. Dou,⁴ X. L. Wang,^{4,a)} and J. M. Chen^{1,a)}

¹National Synchrotron Radiation Research Center, Hsinchu 30076, Taiwan

²Department of Physics, National Tsing Hua University, Hsinchu 30013, Taiwan

³Institute of Physics, Academia Sinica, Taipei 11529, Taiwan

⁴Institute for Superconducting and Electronic Materials, Australian Institute of Innovative Materials, University of Wollongong, North Wollongong, NSW 2500, Australia

(Received 24 October 2012; accepted 16 January 2013; published online 30 January 2013)

We explored the orbital structure of FeTiO₃ with polarization-dependent x-ray absorption spectra complemented with electronic structure calculations. The electronic structure, near the bottom of conduction band, is composed of O 2*p* and Ti 3*d* orbitals. Ti 3*d*/4*p* hybridization dominantly lies on the *ab* plane. The highly delocalized Ti 4*p* orbital might hybridize with O 2*p* orbital and even extend to the next-neighbor Fe atom whereby establishing a linear orbital combination of Ti-O-Fe. A clear picture of the orbital construction in FeTiO₃ will help to elucidate the paths of pressure-induced charge transfer and other physical or magnetic characteristics. © 2013 American Institute of Physics. [<http://dx.doi.org/10.1063/1.4789992>]

FeTiO₃ ilmenite is a mineral existing widely in terrestrial metamorphic and igneous rocks, from the upper mantle to depths about 400 km, at which it suffers pressures 12–13 GPa.¹ Because the oxidation state of iron is highly sensitive to the external environment, FeTiO₃ can thus provide significant information about the history of the terrestrial weather on the crust and the pressure in the mantle.^{2,3}

A valence fluctuation of Fe and Ti in FeTiO₃ is an important phenomenon, especially under extreme conditions. Charge re-distribution, Fe²⁺Ti⁴⁺ to Fe³⁺Ti³⁺, in FeTiO₃ under high pressure was evident in Mössbauer spectra.^{4,5} To deduce the mechanism of charge re-distribution, several researchers focused on the variation of the local structure of FeTiO₃ under high pressure. Figure 1 shows the crystal structure of FeTiO₃, Fe and Ti alternate with cations ordering as Fe-Ti-V-Ti-Fe (V: vacant site) along the rhombohedral axis, *c*, of the crystal.⁶ Metal-metal interaction through the shared face of two adjacent octahedra was expected when external pressure was applied.⁷ Inter-valence charge transfer would be allowed as the *d* orbitals (of Fe and Ti) extend their lobes across the shared face, as path 1 in Fig. 1. Agui *et al.*⁸ also proposed an existence of inter-metallic charge transfer via a direct Ti 3*d* – Fe 3*d* interaction on a basis of resonant inelastic soft-x-ray inelastic-scattering spectra complemented with full-multiplet calculations, but the distribution of electron density deduced from x-ray-diffraction shows a decreased density of charge along a direct Fe-Ti connection, across the shared face, with increasing pressure.⁹ Direct charge transfer via Fe and Ti atoms along the *c* axis seems unlikely. On the other hand, based on the single-crystal diffraction study of FeTiO₃ by Yamanaka, a charge density along both Fe-O and Ti-O bonds increased with increasing pressure.⁹ One thus can expect a possible path of inter-valence charge transfer in FeTiO₃ ilmenite along Fe1-O-Ti1

(path 2) or Fe2-O-Ti1 (path 3) as shown in Fig. 1. Wu *et al.*⁵ proposed similar charge transfer pathway, but no experimental data can evidence this hypothesis. Up on the above results with opposite views, the detailed path of pressure-induced charge transfer in FeTiO₃ remains uncertain.

Associated with charge transfer path closely related to orbital connection, a comprehensive understanding of the orbital structure in FeTiO₃ is a crucial step towards unveiling the nature of charge transfer. Additionally, a clear picture of orbital construction will also serve to elucidate the physical properties of FeTiO₃, such as the anisotropic conductivity and the magnetoelectric coupling phenomena.^{10,11} These properties attract much attention, but there has been little investigation of the orbital structure of FeTiO₃.

In this work, we explored the orbital structure of FeTiO₃ in detail with the polarization-dependent x-ray absorption spectra and electronic structure calculations. The O *K*-edge spectra indicate the orbital hybridization between O 2*p* and a cation orbital, characterizing the orbital structure of FeTiO₃ near the bottom of the conduction band. The Ti *K*- and Fe

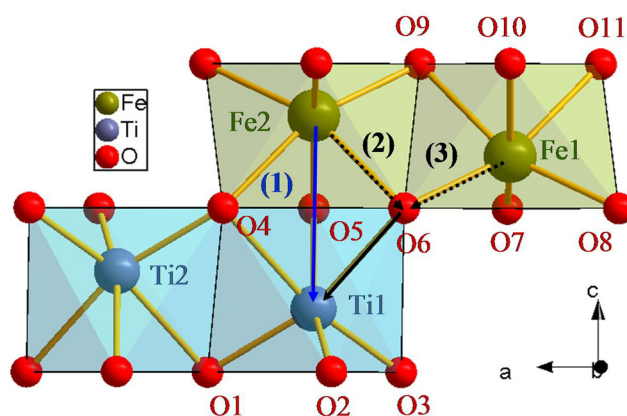


FIG. 1. The structure of FeTiO₃ with possible charge transfer paths in FeO₆ and TiO₆ octahedras.

^{a)} Authors to whom correspondence should be addressed. Electronic addresses: jmchen@nsrrc.org.tw and xiaolin@uow.edu.au.

K-edges spectra clearly show a highly anisotropic hybridization of the $3d/4p$ orbitals and asymmetric atomic bonding. This work accordingly establishes a clear picture of the orbital construction in FeTiO_3 .

FeTiO_3 single crystals were synthesized with a four-mirror floating-zone method. The rhombohedral structure, R-3, of single-crystalline FeTiO_3 was characterized with four-axis x-ray diffraction spectroscopy according to which a periodic diffraction pattern was identified (ICSD #9805). Polarization-dependent x-ray absorption near-edge structure (XANES) spectra were processed in National Synchrotron Radiation Research Center (NSRRC) in Taiwan. XANES spectra dependent on polarization, with electric field vector E perpendicular or parallel to the ab plane, were recorded by controlling the angle between the incident beam of the x-rays and the surface normal of the sample. The Ti K-edge spectra were recorded at wiggler beamline 17C1. Fluorescence emitted from the sample was collected with a Lytle detector. Polarization dependent O K-edge XANES spectra were recorded at beamline BL11A1 (dragon). The measurements were performed in an ultrahigh-vacuum (UHV) chamber. To avoid surface contamination and to probe the electronic structure precisely, the single-crystalline FeTiO_3 was cleaved within the UHV chamber to obtain a clean surface. Signals were then recorded in the total-electron-yield mode on measuring the sample drain current.

Figure 2(a) shows polarization-dependent O K-edge XANES spectra of FeTiO_3 . The spectra display large spectral variation depending on the polarization vector E perpendicular ($E//c$) or nearly parallel ($E//ab$ plane) to the ab -plane. To identify precisely the corresponding orbitals in the O K-edge spectra, we perform the electronic structure calculations with the accurate full-potential projected augmented wave method as implemented in the VASP package within the generalized gradient approximation (GGA) as well as the GGA plus Hubbard U (GGA+U) scheme.^{12–15} The material FeTiO_3 was simulated in the supercell approach under structure optimizations based on the experimental lattice structure.⁶ The calculations were carried out over a $13 \times 13 \times 4$ Monkhorst-Pack k-point mesh in the irreducible Brillouin zone using 54880 plane waves with cut-off energy of 400 eV. On-site Coulomb energy $U=5.5$ eV and exchange parameter $J=0.25$ eV were used for Fe ions to explore the correlation effects in $3d$ orbitals, whereas we use $U=1$, $J=0.1$ eV for Ti ions due to the nearly empty $3d$ orbitals. Results are well consistent with that proposed by Wilson *et al.*⁶ using the modified Becke's three parameter hybrid functional (B3LYP), in which both the Hartree-Fock (HF) and density functional theory (DFT) were adopted. The valence band is mainly composed of O $2p$ and Fe $3d$ orbitals (not shown) while the conduction band arises from the contribution of O $2p$, Ti $3d$, and Fe $3d$ orbitals. Fig. 2(b) presents the calculated density of states of FeTiO_3 focusing on the region of the conduction band. Results indicate that Ti $3d$ orbital, divided into the low lying t_{2g} and high lying e_g states under crystal field, contributes mainly to the electronic structure at about 2–3 eV and 4.2–5.2 eV relative to the Fermi energy, respectively. In D_{3d} symmetry, trigonal distortion of the TiO_6 octahedra further splits the t_{2g} state into a non-degenerated a_{1g} and a doubly degenerated e_g^π sub-states,

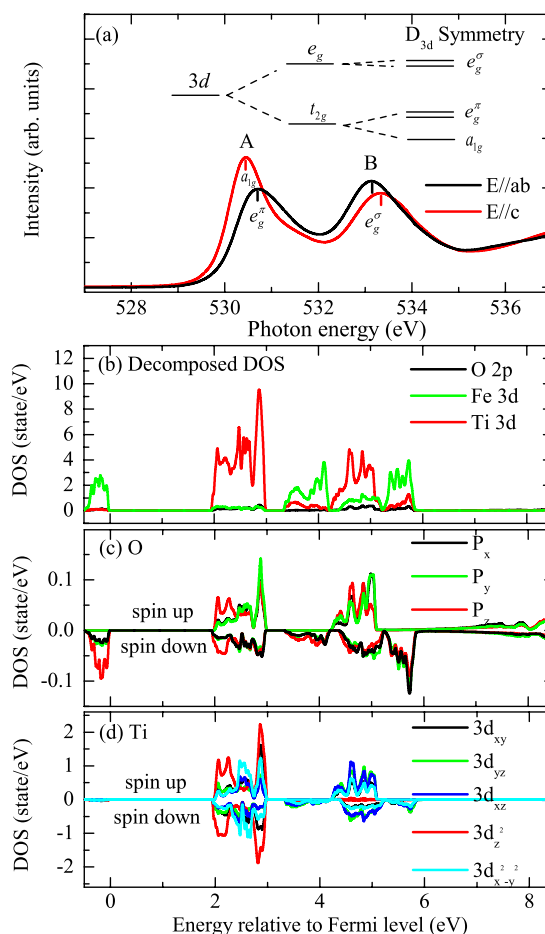


FIG. 2. (a) Polarization-dependent O K-edge XANES spectra of FeTiO_3 . (b) Calculated decomposed density of state. (c) O $2p$ projected density of states. (d) Ti $3d$ projected density of states.

while the e_g state remains doubly degenerated, now called e_g^σ . According to the splitting levels shown in the upper of Fig. 2(a), the features in the O K-edge spectra can be well assigned. The intense feature A, in the polarization dependent O K-edge XANES spectra of FeTiO_3 , situated at a relative lower energy for $E//c$ than for $E//ab$, mainly reflects a strong hybridization between O $2p$ and Ti $3d$ (a_{1g}) orbitals lying near the c axis. Result is further evidenced by the projected density of states of O $2p$ and Ti $3d$ orbitals as shown in Figs. 2(c) and 2(d), respectively. As noted, the O $2p_z$ state, close to the c axis, is significantly situated at a relative lower energy, coincided with Ti $3d_{z^2}$ (a_{1g}) state. That clearly indicates the strong O $2p_z$ – Ti $3d$ (a_{1g}) hybridization near the c axis. The a_{1g} state lying close to the c axis, exhibited in this study, is consistent with the reference.⁴ Feature B in the polarized O K-edge spectra is attributed to the transition of electron from O $1s$ to O $2p$ -Ti $3d$ (e_g) hybridized state. The intensity of feature B significantly greater for $E//ab$ than for $E//c$ then reflects the stronger hybridization between O $2p$ and Ti $3d$ e_g orbitals lying near the ab plane. According to ligand-field theory, e_g orbitals of Ti atoms point directly toward the O ligands, and t_{2g} orbitals are situated between them.¹⁶ Ti1-O1, O2, O3 bonds, with larger projected vectors in the ab plane, thus reflect stronger hybridization between O $2p$ and Ti $3d$ e_g orbitals in the ab plane, in compared with Ti1-O4, O5, O6 bonds. The inter-atomic distances between

Ti1-O1, O2, O3 atoms are correspondingly smaller than those between Ti1-O4, O5, O6 atoms.

From the calculated decomposed density of states, Fe 3*d* bands contribute predominantly to the electronic structure of FeTiO₃ at 3.3–4.2 eV and 5.2–5.8 eV, relative to the Fermi energy, but the corresponding characteristic is suppressed in the polarization-dependent O *K*-edge XANES spectra of FeTiO₃. The condition indicates that hybridization between O 2*p* and Fe 3*d* bands is weak, consistent with the result in the literature.⁵ The oxidation state of Fe ions in FeTiO₃ ilmenite has been identified as +2 according to Fe *L*_{2,3} edge XANES spectra¹⁷ and *K*-edge spectra (discussed below); charge transfer from O²⁻ to Fe²⁺ is hence unlikely, corresponding to the weak hybridization between O 2*p* and Fe 3*d* bands in FeTiO₃.

To investigate further the orientation of the orbital structure, we probed the polarization-dependent Ti *K*-edge XANES spectra of FeTiO₃, as shown in Figure 3(a). We observe a substantial difference in the pre-edge region and the near-edge region with polarizations *E* perpendicular or parallel to the *ab* plane. In the *K*-edge XANES spectra of transition metals, such as Ti¹⁸ or Fe¹⁹ or Co,^{19,20} the absorption features in the pre-edge region are attributed to a 1*s*-3*d* quadrupole transition (forbidden) whereas the main feature in the near-edge region is attributed to a 1*s*-4*p* dipole transition (allowed). Prominent features observed in the pre-edge region of *K*-edge XANES spectra are associated with the distorted geometry of MO₆ (M = transition metals) corresponding to direct M 3*d*-4*p* hybridization or an inter-site M 3*d*-4*p*

hybridization mediated via the intervening O 2*p* orbitals. Discernible in Fig. 3(a), we observe a pronounced feature, labeled A, in the pre-edge region of Ti *K*-edge XANES spectra of FeTiO₃, especially for polarization *E*//*ab*. This feature is well reproduced with the FDMNES calculations with only the allowed dipole transition, as shown in Fig. 3(b). The hybridization of Ti 4*p* and Ti 3*d* orbitals hence occurs predominantly in the *ab* plane.

In Fig. 3(a), we also observe three features, labeled C, D, and E, in the near-edge region of the Ti *K*-edge spectra of FeTiO₃. The near-edge feature might reflect the hole state in the Ti 4*p* orbitals whereas the oscillatory features are the result of multiple scattering contributions of absorbing atoms. Feature C is intense for a polarization parallel to the *c* axis whereas features D and E are prominent for a polarization parallel to the *ab* plane. This phenomenon reflects the relation $\Delta E \propto 1/d^2$ for a XANES resonance, in where ΔE denotes an energy difference of absorption feature relative to the ionization threshold and *d* represents the corresponding interatomic distance.²¹ The observed features in the Ti *K*-edge near-edge spectra of FeTiO₃ at greater energy for *E*//*ab* and at smaller energy for *E*//*c* are then related to the smaller inter-atomic distance in the *ab* plane and the larger one in the *c* direction, respectively.

Figure 4(a) shows the polarization-dependent Fe *K*-edge XANES spectra of FeTiO₃. The features in the pre-edge region show a weak dependence on polarization, whereas the features in the near-edge region vary strongly with the polarization of incident X-ray. As indicated, the features in the pre-edge region are not pronounced, associated with the slightly asymmetric geometry of FeO₆ octahedra with the small difference of bond lengths between Fe-O6, O7, O8 (2.07 Å) and Fe-O9, O10, O11 (2.20 Å). Accordingly, a weak Fe 3*d*-4*p* hybridization is represented. In the near-edge region, an absorption feature about 7131 eV vanishes gradually when the polarization is varied from *E*//*ab* plane to *E*//*c* axis. Anisotropic axial lengths and bond distances in the rhombohedral structure of FeTiO₃ would contribute to this result. The absorption feature at a greater energy reflects the multiple scattering of absorbing atoms with a smaller distance. The local structure around the Fe atoms with the shorter bond projected in the *ab* plane consequently leads to

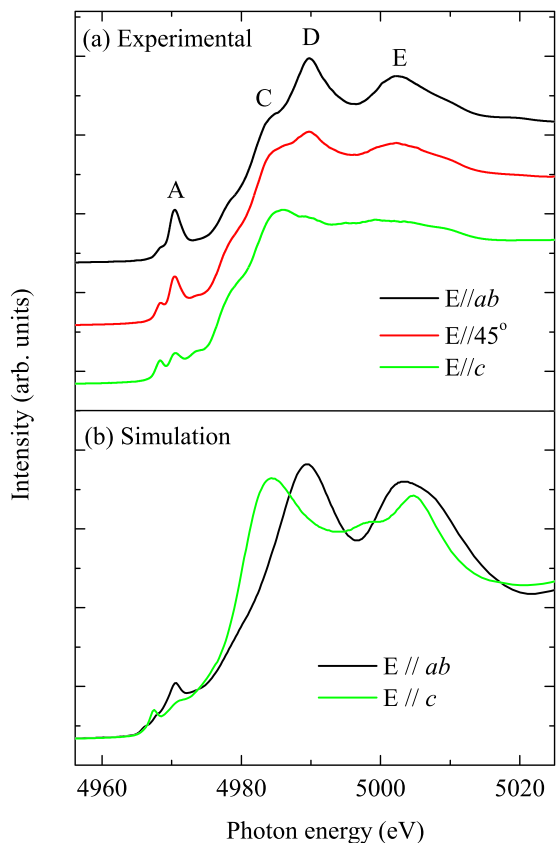


FIG. 3. (a) Polarization-dependent Ti *K*-edge spectra of FeTiO₃. (b) Simulated Ti *K*-edge spectra with FDMNES code with a radius of 5 Å, corresponding to 48 atoms. (Ref. 24).

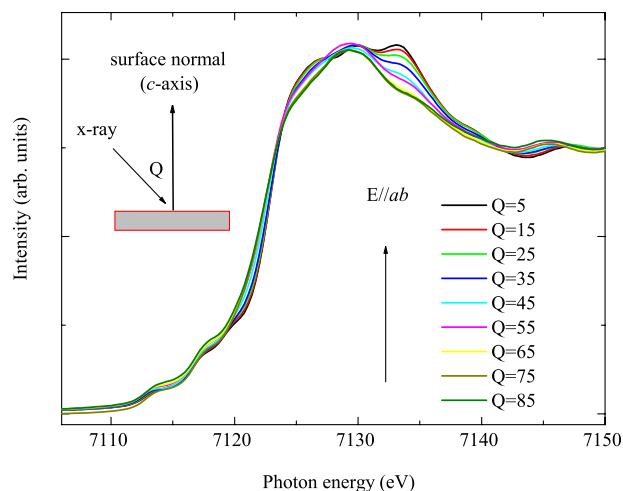


FIG. 4. Polarization-dependent Fe *K*-edge spectra of FeTiO₃.

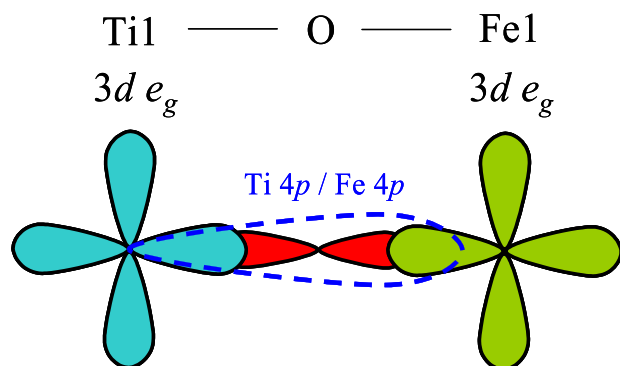


FIG. 5. Sketch of orbital connection between Ti1-O-Fe1.

an absorption feature at 7131 eV in the polarization-dependent Fe *K*-edge XANES spectra of FeTiO₃, whereas the Fe atoms with a longer bond in the *c*-axis direction would contribute to the absorption feature at smaller energy.

As evidenced in the O *K*-edge XANES spectra and electronic-structure calculations shown in Fig. 2, the electronic structure of FeTiO₃ involves O *2p* and Ti *3d* orbitals near the bottom of conduction band. O *2p*-Ti *3d* hybridized bands thus play an essential role in the orbital structure serving charge transfer. The Ti *K*-edge XANES spectra, shown in Fig. 3, further evidence the Ti *3d*-*4p* hybridized orbitals predominantly lying in the *ab* plane. Because of the *4p* orbital of transition metals is broad and highly delocalized, we thus expect that the Ti *4p* orbital to make an additional contribution to the orbital connection in the *ab* plane. Based on the existence of a direct Ti *3d*-Fe *3d* interaction, demonstrated with resonant inelastic soft x-ray inelastic-scattering measurements,⁸ the highly delocalized Ti *4p* orbitals might hybridize with the *2p* orbital of the neighboring O atoms and even extend to the next-neighbor Fe atoms, as for the Mn *4p* states displayed in LaMnO₃.^{22,23} A linear orbital combination of Ti1-O-Fe1 is then established, as in the sketch in Figure 5. That path (path 3, shown in Fig. 1) might thus serve for charge transfer when pressure is applied. We cannot here exclude a contribution of Fe *3d* and *4p* orbitals to the orbital connection. However, because of weak O *2p*-Fe *3d* hybridization and weak Fe *3d*-*4p* hybridization, as indicated in Figs. 2 and 5, the contribution of Fe *3d* and *4p* orbitals to the orbital connection is expected to be minor.

In conclusions, this study exposes the orbital structure of FeTiO₃ ilmenite in detail with the polarization-dependent

x-ray absorption spectra complemented with calculations of electronic structure. A clear picture of orbital construction of FeTiO₃ ilmenite, according to this study, will be fundamental to elucidate precisely its electronic and magnetic properties.

We thank NSRRC staff for their technical support. This work is supported by NSRRC and National Science Council of Republic of China (Grant No. NSC 99-2113-M-213-006-MY3) and supported in part by Australian Research Council through a discovery Project DP0987190 and Scientific visit Grant from Australian Academy of Science.

¹S. E. Haggerty and V. Sautter, *Science* **248**, 993 (1990).

²C. Palmer, *Am. J. Sci.* **28**, 353 (1909).

³I. E. Grey and A. F. Reid, *Am. Mineral.* **60**, 898 (1975).

⁴T. Seda and G. R. Hearne, *J. Phys.: Condens. Matter* **16**, 2707 (2004).

⁵X. Wu, G. Steinle-Neumann, O. Narygina, I. Kantor, C. McCammon, S. Pascarelli, G. Aquilanti, V. Prakapenka, and L. Dubrovinsky, *Phys. Rev. B* **79**, 094106 (2009).

⁶N. C. Wilson, J. Muscat, D. Mkhonto, P. E. Ngoepe, and N. M. Harrison, *Phys. Rev. B* **71**, 075202 (2005).

⁷G. Radtke, S. Lazar, and G. A. Botton, *Phys. Rev. B* **74**, 155117 (2006).

⁸A. Agui, T. Uozumi, M. Mizumaki, and T. Käämbre, *Phys. Rev. B* **79**, 092402 (2009).

⁹T. Yamanaka, *J. Synchrotron Rad.* **12**, 566 (2005).

¹⁰C. J. Fennie, *Phys. Rev. Lett.* **100**, 167203 (2008).

¹¹T. Varga, A. Kumar, E. Vlahos, S. Denev, M. Park, S. Hong, T. Sanehira, Y. Wang, C. J. Fennie, S. K. Streiffer, X. Ke, P. Schiffer, V. Gopalan, and J. F. Mitchell, *Phys. Rev. Lett.* **103**, 047601 (2009).

¹²G. Kresse and J. Joubert, *Phys. Rev. B* **59**, 1758 (1999).

¹³G. Kresse and J. Hafner, *Phys. Rev. B* **48**, 13115 (1993).

¹⁴J. P. Perdew and Y. Wang, *Phys. Rev. B* **45**, 13244 (1992).

¹⁵A. I. Liechtenstein, V. I. Anisimov, and J. Zaanen, *Phys. Rev. B* **52**, R5467 (1995).

¹⁶F. M. F. De-Groot, J. C. Fuggle, B. T. Thole, and G. A. Sawatzky, *Phys. Rev. B* **41**, 928 (1990).

¹⁷See supplementary material at <http://dx.doi.org/10.1063/1.4789992> for details of Ti *L*- and Fe *L*-edges spectra of FeTiO₃.

¹⁸S. W. Chen, J. M. Lee, S. Chiang, S. C. Haw, Y. C. Liang, K. T. Lu, C. W. Pao, J. F. Lee, M. T. Tang, and J. M. Chen, *J. Phys. Soc. Jpn.* **80**, 114706 (2011).

¹⁹V. Iota, J. P. Klepeis, C. Yoo, J. Lang, D. Haskel, and G. Srajer, *Appl. Phys. Lett.* **90**, 042505 (2007).

²⁰F. De-Groot, G. Vanko, and P. Glatzel, *J. Phys.: Condens. Matter* **21**, 104207 (2009).

²¹A. Bianconi, E. Fritsch, G. Calas, and L. Petiau, *Phys. Rev. B* **32**, 4292 (1985).

²²H. Hayashi, A. Sato, T. Azumi, Y. Udagawa, T. Inami, K. Ishii, and K. B. Garg, *Phys. Rev. B* **73**, 134405 (2006).

²³F. Bridges, C. H. Booth, M. Anderson, G. H. Kwei, J. J. Neumeier, J. Snyder, J. Mitchell, J. S. Gardner, and E. Brosha, *Phys. Rev. B* **63**, 214405 (2001).

²⁴Y. Joly, *Phys. Rev. B* **63**, 125120 (2001).